Phenomenological description of counterflow superfluid turbulence in rotating containers

D. Jou[1] and M. S. Mongiovì[2]
[1]*Departament de Física, Universitat Autònoma de Barcelona, Catalonia, Spain*
[2]*Dipartimento di Matematica ed Applicazioni, Università di Palermo, Italy*
(Received 25 March 2003; revised manuscript received 23 October 2003; published 18 March 2004)

In this paper a simple equation for the vortex line density describing some of the most relevant observed effects in counterflow superfluid turbulence in ^{4}He in the presence of rotation is proposed. This model is based on a generalization of Vinen's equation which incorporates as additional quantity the angular velocity Ω.

DOI: 10.1103/PhysRevB.69.094513 PACS number(s): 67.40.Vs, 67.40.Bz, 47.27.−i, 05.70.Ln

I. INTRODUCTION

In recent years the study of turbulence in quantum systems has received new attention.[1,2] Here, we consider the turbulence in superfluid ^{4}He, which is the most studied system in this field. Superfluid turbulence in ^{4}He (Refs. 2–5) has been investigated in two physical situations: rotating containers and counterflow experiments. In the first one, the vortex lines are parallel to the rotation axis, whereas in the second one they form a quasi-isotropic tangle. In both situations an extra dissipation beside the one due to viscosity alone is present, which can be represented, macroscopically, by adding a ''mutual friction'' term in the two-fluid equations of motion. From a microscopical point of view, the mutual friction results from the collision of the quasiparticles with the vortex lines.[2–5] The collision cross section is a function of the direction of the roton drift velocity relative to the vortex line: it is a maximum when the roton is travelling perpendicular to this line and a minimum (in fact zero) when the roton moves parallel to the line. The microscopic mechanism is the same in rotating helium II as in counterflow superfluid turbulence. In both cases (rotation only and counterflow only) the vortex array is described by introducing a scalar quantity L, the average vortex line length per unit volume [briefly called *line density* and whose dimensions are $(\text{length})^{-2}$]. In the first case the structure of the vortex lines is an ordered array of lines aligned along the rotation axis, of areal density L_R proportional to the angular velocity Ω of the sample; in this case the line density L equals the areal density L_R:

$$L = L_R = \frac{2\Omega}{\kappa}, \tag{1.1}$$

where κ is the quantum of vorticity ($\kappa = h/m_4$, with h the Planck constant, and m_4 the mass of ^{4}He atom: $\kappa \simeq 9.97\,10^{-4}$ cm^2/s). In the second case, the vortex line structure is a disordered tangle of lines; in this case the vortex line density L is proportional to the square of the counterflow velocity V ($\mathbf{V} = \mathbf{v}_n - \mathbf{v}_s$, $\mathbf{v}_n$, and $\mathbf{v}_s$ being the velocities of the normal and superfluid components):

$$L = L_H = \gamma_H V^2. \tag{1.2}$$

Combined rotation and heat flux is a relatively new area of investigation.[4–7] The interest of combining both situations is great because it turns out, experimentally[6] and numerically,[7] that both effects are not merely additive, but show an interplay between the ordered vortices of rotation and the disordered ones of counterflow. On the other side, the number of papers related to this topic is still very low, in such a way that the subject deserves more attention. Here, we propose a model able to describe some of the main observed features of these phenomena, by a suitable phenomenological generalization of Vinen's equation.[8]

II. BRIEF ACCOUNT OF ESSENTIAL PHENOMENOLOGY IN COMBINED ROTATION AND COUNTERFLOW

The combined rotation and axial counterflow in steady state exhibits a rich set of features in superfluid turbulence. In Ref. 6, Swanson *et al.* experimentally found that in combined situations the effects of rotation and counterflow are not additive. In that work, the experimental observation consisted in measuring the amount of vortex lines present owing to counterflow or rotation alone, and comparing the observed line density with what would be expected if the two sources of vorticity simply added. Their measurements showed that the ordered array of vortex lines produced by steady rotation and the disordered tangle produced by the counterflow do not preserve their identities in a combined experiment. This experimental work has recently been complemented by numerical simulations based on the vortex filament model,[7] which are clarifying as they explicitly illustrate the evolution from an initial set of parallel vortex lines to a final vortex tangle.

In the present study on this intricate behavior, we will consider only the experiments in the range $0.2\ \text{Hz} \leqslant \Omega/2\pi \leqslant 1.0$ Hz and $0 \leqslant V^2 \leqslant 0.2$ cm^2/s^2. The essential experimental observations may be summarized as follows. Assume that the container is rotating at a given angular speed Ω and that an increasing heat flow (corresponding to a counterflow velocity V) parallel to the rotation axis, is imposed. Then one finds the complete absence of the laminar regime, and the presence of two critical velocities V_{c1} and V_{c2}, which scale as $\Omega^{1/2}$; more precisely: (a) for $V \leqslant V_{c1}$, with V_{c1} a counterflow-rotation critical velocity, the length L per unit volume of the vortex lines is independent of V and proportional to the angular speed Ω, in particular, $L = 2\Omega/\kappa$, (b) for $V_{c1} \leqslant V \leqslant V_{c2}$, with V_{c2} a second counterflow-rotation critical velocity, one observes a situation similar to (a), but with L independent of V and proportional to Ω, with a slightly different proportionality constant than in the previous situation, (c) for

$V \geqslant V_{c2}$, L increases with V and becomes proportional to V^2 at high values of V.

The two critical counterflow-rotation velocities V_{c1} and V_{c2}, scale as $\Omega^{1/2}$: $V_{c1}=C_1\sqrt{\Omega}$, $V_{c2}=C_2\sqrt{\Omega}$, with $C_1=0.053\ \mathrm{cm\,sec}^{-1/2}$, $C_2=0.118\ \mathrm{cm\,sec}^{-1/2}$. The first transition appears to correspond to the Donnelly-Glaberson instability:[9–11] excitation of helical waves (Kelvin waves) by the counterflow on the vortex lines induced by rotation. The second appears to be a transition to a turbulent disordered tangle, when the ordered array begins behaving as a turbulent tangle of interconnected vortices. According to the numerical simulations in Ref. 7, this second transition takes place through the reconnection of the deformed helical lines when the amplitude of the Kelvin waves becomes of the order of the average vortex separation. In the range of Ω and V considered, the measured values of L are always less than L_H+L_R [L_H and L_R as defined in Eqs. (1.2) and (1.1)], and the deviation increases with V and Ω. In the limit of large heat flux and slow rotation, the tangle appears to be ''polarized'' to accomplish the rotation. The effective polarization increases with rotation.

The dynamics of polarization has been the object of recent studies. In Ref. 12, in the case of purely counterflow experiments, Lipniacki proposed a system of coupled evolution equations for L and for a vector $\mathbf{I}$, characterizing the anisotropy of the tangle, defined as

$$\mathbf{I}=\frac{\langle \mathbf{s}'\times\mathbf{s}''\rangle}{\langle|\mathbf{s}''|\rangle}, \tag{2.1}$$

where $\mathbf{s}=\mathbf{s}(\xi,t)$, ξ being the arclength of the vortex line. In the present study of the superfluid turbulence in rotating containers, we will suppose that the anisotropy vector $\mathbf{I}$ assumes its steady-state value $\mathbf{I}^{(H,\Omega)}=\mathbf{I}(V,\Omega)$, collinear to the rotation axis and to the counterflow velocity $\mathbf{V}$.

III. EVOLUTION OF *L*. DERIVATION OF A GENERALIZED VINEN'S EQUATION IN THE PRESENCE OF ROTATION

To describe L as a function of V and Ω, we resort to a modification of Vinen's equation. In Vinen's model,[8] the counterflow velocity V appears as an external fixed parameter that remains constant in the evolution of the vortex tangle. Vinen assumes that the time derivative of L is composed of two opposite contributions

$$\frac{dL}{dt}=\left[\frac{dL}{dt}\right]_f-\left[\frac{dL}{dt}\right]_d, \tag{3.1}$$

where subscripts f and d denote formation and destruction of vortices per unit of time, respectively. The growth of the line density is due to the mutual friction force $\mathbf{f}$, the decay is originated by a cascadelike process of vortex breakup, due to the vortex reconnection, with formation of smaller and smaller loops, which in the final stage of the cascade contract and are lost.

Vinen supposes that the growth rate of L depends on L and on the mutual friction force $\mathbf{f}$ (i.e., on V). Dimensional analysis leads to the equation:[8,13]

$$\left[\frac{dL}{dt}\right]_f=\kappa L^2\phi_f\left[\frac{V}{\kappa L^{1/2}}\right], \tag{3.2}$$

where ϕ_f is a dimensionless function, which depends on the dimensionless combination $V\kappa^{-1}L^{-1/2}$. By analogy with the growth of a vortex ring, he assumes that ϕ_f is linearly dependent on its argument, obtaining[8,13]

$$\left[\frac{dL}{dt}\right]_f=\alpha V L^{3/2}, \tag{3.3}$$

with α a dimensionless constant.

The form of the $[dL/dt]_d$ term, responsible for the vortex decay, was determined in analogy with classical turbulence. Assuming that the vortex breakup is analogous to a Kolmogorov cascade, Vinen obtained[8,13]

$$\left[\frac{dL}{dt}\right]_d=-\beta\kappa L^2 \quad \text{with} \quad \beta=\frac{\chi_2}{2\pi}, \tag{3.4}$$

being χ_2 a dimensionless constant of the order of unity. Substituting Eqs. (3.3) and (3.4) in Eq. (3.1) one obtains the well known Vinen's equation[8]

$$\frac{dL}{dt}=\alpha V L^{3/2}-\beta\kappa L^2. \tag{3.5}$$

The steady state solution of Eq. (3.5) is

$$L_H=\frac{\alpha^2}{\beta^2\kappa^2}V^2, \tag{3.6}$$

in accord with Eq. (1.2).

To derive an evolution equation for L in the presence of counterflow and rotation, we must take into account that the formation of vortex lines is due not only to V but also to Ω. We model the destruction contribution, as Vinen, with Eq. (3.5), and the production contribution with a term depending on V and Ω (as well as on κ and L). When the heat flux and the rotation are simultaneously present, there appears a complex interaction between both processes in the formation and destruction of vortices. Here, we include these effects supposing that the function ϕ_f depends simultaneously on the two only (independent) dimensionless combinations of V, Ω, κ, and L:

$$\left[\frac{dL}{dt}\right]_f=\kappa L^2\phi_f\left[\left(\frac{V}{\kappa L^{1/2}}\right),\left(\frac{\Omega}{\kappa L}\right)^{1/2}\right]. \tag{3.7}$$

Note that we use as arguments of the function ϕ_f a term in V and a term in $\Omega^{1/2}$; this is motivated by the dependence of the steady-state values of L, in counterflow only and in rotation only, on V and on Ω [see Eqs. (1.2) and (1.1), respectively], and by the observation that the microscopic mechanism responsible of the growth of vortices (the mutual friction force) is the same in rotating helium II and in superfluid turbulence.

For the function ϕ_f we will choose a quadratic dependence on its variables

$$\phi_f = \alpha_1 \frac{V}{\kappa L^{1/2}} + \alpha_2 \left(\frac{\Omega}{\kappa L}\right)^{1/2} + \alpha_3 \frac{\Omega}{\kappa L} + \alpha_4 \frac{V}{\kappa L^{1/2}} \left(\frac{\Omega}{\kappa L}\right)^{1/2}, \tag{3.8}$$

where α_i are dimensionless constants. The term in V^2 has been omitted because the values of V considered in this paper are not too high.

Observe that, if we had limited Eq. (3.8) to the linear terms, the effects of V and Ω would have been merely additive. The choice (3.9) is motivated by the fact (outlined in Sec. II) that experiments on combined rotation and counterflow show that, in the considered regimes of V and Ω, the total vortex line density L is much less than $L_H + L_R$. This feature increases with V and with Ω. Therefore, the rotation facilitates the vortex formation, in the absence or for small counterflow velocities, but it hinders their lengthening for high values of V and Ω. To take into account the experimental results, the coefficients α_1 and α_2 are positive coefficients, while the coefficients α_3 and α_4 may become negative for relatively high values of Ω. In the following we will make this assumption, since we are in this range of Ω. Thus, we obtain

$$\left[\frac{dL}{dt}\right]_f = \alpha_1 V L^{3/2} + \alpha_2 \sqrt{\kappa\Omega} L^{3/2} + \alpha_3 \Omega L + \alpha_4 V \frac{\sqrt{\Omega}}{\sqrt{\kappa}} L. \tag{3.9}$$

We will show that Eq. (3.9) is a good approximation of the unknown function ϕ_f, in the range of V and Ω considered in this paper.

Observe that, from the experimental observations reported in Ref. 5, which we have briefly recalled in Sec. II (see also Sec. VI), one deduces that the evolution of L seems to depend on the anisotropy of the tangle; obviously, in a complete dynamical model, also the anisotropy vector **I** will satisfy an evolution equation, depending on V and on Ω. The experimental observations imply that the evolution equations of L and **I** are not independent of each other. In this work we will limit to study the evolution for L; to take into account of the polarization of the tangle, we will suppose that the dimensionless coefficients α_i can depend on the anisotropy factor **I**. Further, they can depend on the temperature T; i.e., $\alpha_i = \alpha_i(T, \mathbf{I}^{(H,\Omega)})$, where $\mathbf{I}^{(H,\Omega)}$ is the steady-state value of the anisotropy vector **I** in combined counterflow and rotation.

Of course, it would be convenient to have a microscopic interpretation for each of the new terms appearing in Eq. (3.9), but, to our knowledge, this is not yet available in current models, though the very recent numerical investigations in Ref. 7 may be useful to get a detailed microscopic understanding of each term in the near future. We hope that the present macroscopic phenomenological modelization may stimulate the microscopic interpretation, by underlying the influence of different several contributions.

Substituting Eqs. (3.4) and (3.9) in Eq. (3.1), we obtain

$$\frac{dL}{dt} = -\alpha_3 \kappa L^2 + [\alpha_1 V + \beta_2 \sqrt{\kappa\Omega}] L^{3/2} - \left[\beta_1 \Omega + \beta_4 \frac{V\sqrt{\Omega}}{\sqrt{\kappa}}\right] L, \tag{3.10}$$

where $\beta = \alpha_3$, $\alpha_2 = \beta_2$ and $\alpha_3 = -\beta_1$, $\alpha_4 = -\beta_4$. We have thus new terms not present in Vinen's equation. These terms are absent in the absence of rotation, thus recovering Vinen's original equation (3.5).

IV. ANALYSIS OF THE GENERALIZED VINEN'S EQUATION IN SOME SITUATIONS

In this section we will show that Eq. (3.10) allows us to describe most of the phenomenology mentioned in Sec. II. To do that we consider both situations: rotation only and combined rotation and counterflow. Counterflow only need not be considered, as in this case Eq. (3.10) reduces to Vinen's one, as already said.

Case 1: Rotation only. For $V = 0$ and $\Omega \neq 0$ equation (3.10) becomes

$$\frac{dL}{dt} = -\alpha_3 \kappa L^2 + \beta_2 \sqrt{\kappa\Omega} L^{3/2} - \beta_1 \Omega L. \tag{4.1}$$

This equation admits the only stable stationary solution

$$L_R^{1/2} = \left[\frac{\beta_2}{2\alpha_3} + \sqrt{\frac{\beta_2^2 - 4\alpha_3\beta_1}{4\alpha_3^2}}\right] \sqrt{\frac{\Omega}{\kappa}}, \tag{4.2}$$

where we must put

$$\frac{\beta_2 + \sqrt{\beta_2^2 - 4\alpha_3\beta_1}}{2a_3} = \sqrt{2}, \tag{4.3}$$

to agree with Eq. (1.1). Then, one has L proportional to the angular velocity Ω, according to theoretical prediction and experimental results.

Case 2: Combined rotation and counterflow. In the presence of rotation and counterflow, the stationary solutions of Eq. (3.10) are solutions of the following second-order algebraic equation in the unknown $L^{1/2}$:

$$-\alpha_3 \kappa L + [\alpha_1 V + \beta_2 \sqrt{\kappa\Omega}] L^{1/2} - \beta_1 \Omega - \beta_4 \frac{V\sqrt{\Omega}}{\sqrt{\kappa}} = 0. \tag{4.4}$$

Looking at Fig. 3 of Ref. 6 (which shows L as function of V^2), we note that L is almost independent on V for $V < V_{c2}$, with a step change around V_{c1} (in other words, for $V < V_{c1}$, L as a function of V^2 is a horizontal line with a small step in V_{c1}). However, there is a variation of the slope near V_{c2}. We will concentrate in this section on the change near V_{c2}, and will differ the analysis around V_{c1} to Sec. VI. In the concluding Sec. VII, we will comment the microscopic differences between both transitions, which justify this different analysis, on the basis on the information provided by the recent numerical simulation of Ref. 7.

Equation (4.4) (which describes $L^{1/2}$ as function of V) has this behavior in the limiting case in which

$$\frac{\beta_1}{\alpha_3}=\frac{\beta_4}{\alpha_1}\left(\frac{\beta_4}{\alpha_1}-\frac{\beta_2}{\alpha_3}\right). \tag{4.5}$$

Under hypothesis (4.5), the solutions of Eq. (3.10) can be written

$$L^{1/2}=\frac{\beta_4}{\alpha_1}\sqrt{\frac{\Omega}{\kappa}}, \tag{4.6}$$

$$L^{1/2}=\overline{\gamma}V+\left(\frac{\beta_2}{\alpha_3}-\frac{\beta_4}{\alpha_1}\right)\sqrt{\frac{\Omega}{\kappa}}, \tag{4.7}$$

where we have put

$$\overline{\gamma}=\frac{\alpha_1}{\alpha_3\kappa}. \tag{4.8}$$

Further, observing that the experimental data show that the quantity $(\beta_2/\alpha_3)-(\beta_4/\alpha_1)$ appearing in Eq. (4.7) must be positive, one deduces from Eq. (4.5) that both the coefficients $\beta_1=-\alpha_3$ and $\beta_4=-\alpha_4$ must be positive, and contribute to hinder the lengthening of the vortices.

Equation (4.6) represents a family of straight lines parallel to the V axis, which scale with $\sqrt{\Omega}$. Making use of Eq. (1.1), Eq. (4.6) can be written, for further convenience, as

$$L^{1/2}=mL_R^{1/2}, \quad \text{where} \quad m=\frac{\beta_4}{\sqrt{2}\alpha_1}; \tag{4.9}$$

some details about m will be commented in Sec. VI. Equation (4.7) represents a family of straight lines with the same slope, independent of Ω. In order to study the stability of solutions (4.6) and (4.7), we write the evolution equation for the perturbation δL, which is

$$\frac{d\,\delta L}{dt}=\left[-2\alpha_3\kappa L+\frac{3}{2}(\alpha_1 V+\beta_2\sqrt{\kappa\Omega})L^{1/2}+\beta_1\Omega-\beta_4\frac{V\sqrt{\Omega}}{\sqrt{\kappa}}\right]\delta L. \tag{4.10}$$

Substituting Eq. (4.6) in Eq. (4.10) and using Eq. (4.5), we obtain

$$\frac{d\,\delta L}{dt}=\frac{\beta_4}{2}\left[\sqrt{\frac{\Omega}{\kappa}}V-\frac{\alpha_3}{\alpha_1}\left(2\frac{\beta_4}{\alpha_1}-\frac{\beta_2}{\alpha_3}\right)\Omega\right]\delta L. \tag{4.11}$$

Thus we see that the prefactor in Eq. (4.10) is negative for counterflow velocities V lower than

$$V_{c2}=\frac{1}{\overline{\gamma}}\left[2\frac{\beta_4}{\alpha_1}-\frac{\beta_2}{\alpha_3}\right]\sqrt{\frac{\Omega}{\kappa}} \tag{4.12}$$

[corresponding to the point of interception of the straight lines (4.6) and (4.7)]. Consequently Eq. (4.6) is stable for $0<V<V_{c2}$. A similar calculation [i.e., introducing Eq. (4.7) in Eq. (4.10) and studying the sign of the prefactor] shows that, for values of V higher than V_{c2}, the solution (4.7) is stable. Therefore V_{c2} represents the critical counterflow-rotation velocity, mentioned in point (c) of Sec. II, which characterizes the transition to a turbulent disordered tangle. As we see, this critical velocity scales as $\sqrt{\Omega}$, in agreement with experimental observations. The critical velocity V_{c1} will be commented in Sec. VI.

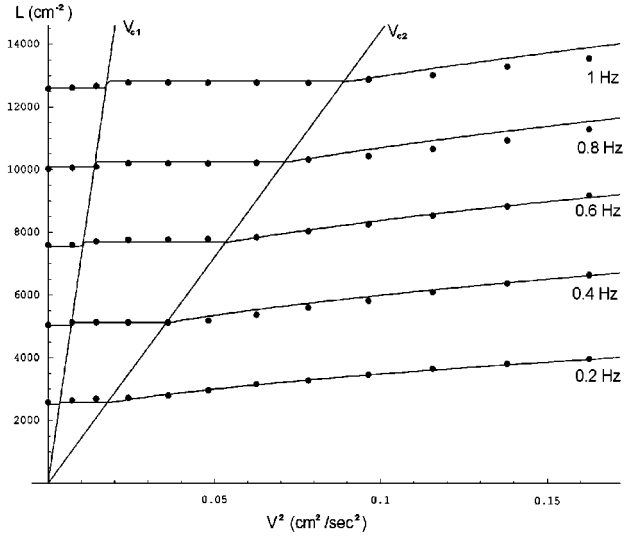

FIG. 1. Vortex line density L, shown as function of V^2 [Eqs. (4.13) and (4.14), with m expressed by Eq. (6.1), and $N=100$]. The equations of the straight lines are, respectively, $L=L_H V^2/V_{c1}^2$ and $L=L_H V^2/V_{c2}^2$. Experimental data are from Ref. 6.

Finally, we observe that Fig. 3 of Ref. 6 (and our Fig. 1) shows the values of L as function of V^2. Equations (4.6) and (4.7) in the variables (L,V^2), become

$$L=\left[\frac{\beta_4}{\alpha_1}\right]^2\frac{\Omega}{\kappa}=m^2\frac{2\Omega}{\kappa}, \tag{4.13}$$

$$L=\overline{\gamma}^2V^2+\left[\frac{\beta^4}{\alpha_1}-\frac{\beta_2}{\alpha_3}\right]^2\frac{\Omega}{\kappa}+2\overline{\gamma}\left(\frac{\beta_4}{\alpha_1}-\frac{\beta_2}{\alpha_3}\right)V\sqrt{\frac{\Omega}{\kappa}}, \tag{4.14}$$

which are respectively stable for $V^2<V_{c2}^2$ and for $V^2>V_{c2}^2$. Observe that the value of the coefficient $\overline{\gamma}$ differs from the coefficient γ_H, introduced in Eq. (1.2), which characterizes the stationary solution in the presence of counterflow only, because the coefficients α_i depend on the anisotropy vector **I**, which is different in the two situations.

V. EXPERIMENTAL RESULTS. DISCUSSION

In this section, we will show that the experimental data on the steady states of L may allow us to determine the four dimensionless quantities

$$\frac{\alpha_1}{\alpha_3}, \quad \frac{\beta_1}{\alpha_3}, \quad \frac{\beta_2}{\alpha_3}, \quad \frac{\beta_4}{\alpha_1}. \tag{5.1}$$

Indeed Eq. (4.12) indicates the value of the counterflow-rotation critical velocity V_{c2}; Eqs. (4.13) and (4.14) provide the value of L for $V_{c1}<V<V_{c2}$ and $V>V_{c2}$, respectively, and allow us to obtain β_4/α_1, β_2/α_3 and α_1/α_3, respec-

tively. Equation (4.5) furnishes the value of the coefficient β_1/α_3 as function of α_1/α_3, β_2/α_3, and β_4/α_1. The coefficient α_3, which controls the rate of evolution of L, cannot be determined by the knowledge of the stationary solutions. We will choose for this coefficient, the theoretical value obtained by Vinen.

At first, we recall that experimental results show that the second counterflow-rotation critical velocity V_{c2} is proportional to $\sqrt{\Omega}$; therefore, from Eq. (4.12), we can write

$$V_{c2}=\frac{1}{\overline{\gamma}}\left[\frac{2\beta_4}{\alpha_1}-\frac{\beta_2}{\alpha_3}\right]\sqrt{\frac{\Omega}{\kappa}}=C_2\sqrt{\Omega}. \tag{5.2}$$

The value of C_2 being known from experimental data, we obtain

$$\frac{1}{\overline{\gamma}}\frac{1}{\sqrt{\kappa}}\left[\frac{2\beta_4}{\alpha_1}-\frac{\beta_2}{\alpha_3}\right]=C_2=0.118 \ \ \mathrm{cm\,sec}^{-1/2}. \tag{5.3}$$

From Eq. (4.7), making use of Eq. (5.3), one obtains

$$L^{1/2}=\overline{\gamma}V+\left[\frac{\beta_4}{\alpha_1}-\overline{\gamma}C_2\sqrt{\kappa}\right]\sqrt{\frac{\Omega}{\kappa}}. \tag{5.4}$$

The value of β_4/α_1 (and of m) can be obtained, using Eq. (4.13), from the experimental values of L in the region $[V_{c1},V_{c2}]$. Figure 3 of Ref. 6 (and our Fig. 1) shows that in this region

$$\frac{L(V_{c2})}{L_R}=m^2=1.018; \tag{5.5}$$

consequently, we will choose

$$m=\frac{\beta_4}{\sqrt{2}\alpha_1}=1.009\rightarrow\frac{\beta_4}{\alpha_1}=1.427. \tag{5.6}$$

It remains only to choose the quantity $\overline{\gamma}$, which characterizes the slope of the straight lines (4.7). Experimental data reported in Fig. 3 of Ref. 6, show that a good choice is

$$\overline{\gamma}=\frac{\alpha_1}{\alpha_3\kappa}=47 \ \ \mathrm{cm\,sec}^{-1/2}\rightarrow\frac{\alpha_1}{\alpha_3}=0.0469. \tag{5.7}$$

Finally, from Eqs. (5.3) and (4.5), we obtain

$$\frac{\beta_2}{\alpha_3}=2.68, \quad \frac{\beta_1}{\alpha_3}=1.78. \tag{5.8}$$

In Fig. 1 we show the results for the vortex line density L to different values of V and Ω, with this four parameters.

We emphasize that the four numerical values (5.6), (5.7), and (5.8), furnish a good approximation to more than 60 experimental data, depending on Ω and V. The coefficient α_3, which controls the rate of the evolution of L, can be identified with the coefficient β introduced by Vinen to take into account the decay of the superfluid turbulence. We may affirm that the model proposed in Eqs. (3.7)–(3.8) for the formation term, in the considered range of values of Ω and V, is a good approximation of a yet unknown microscopic model. However, it does not describe the small step in L near V_{c1}, mentioned in point (b) of Sec. II. We comment on this in the next section.

VI. THE FIRST CRITICAL VELOCITY AND THE ANISOTROPY FACTOR

The model developed in the previous sections [Eq. (3.10)] does not describe, however, the existence of the first critical velocity V_{c1} mentioned in points (a) and (b) of Sec. II in which the value relating L to Ω has a relatively small, but steep change. To do this, we assume that the coefficient m defined in Eq. (4.9) (i.e., β_4) is not properly a constant, but that it depends on Ω and V. In particular, we propose that

$$m=A-B\tanh\left[\frac{\sqrt{k\Omega}}{V}-C\right], \tag{6.1}$$

with A, B, and C constants, in such a way that for $V\ll V_{c1}=(1/C)\sqrt{k\Omega}$, $m\simeq A-B$ and for $V\gg V_{c1}$, $m=A+B$. The constant C is related to V_{c1}, whereas $2B$ gives the size of the step of m near V_{c1}. In fact, if V_{c1} is small, the domain of V in which the transition from $m=A-B$ to $m=A+B$ is produced is very narrow, as observed in experiments.

This assumption for m could seem, at first sight, a merely ad hoc assumption. However, it is reasonably founded in the microscopic ideas about the nature of the transition, already proposed by Donnelly.[4,11] Indeed, it is assumed that for small V, the vortex lines are straight lines parallel to the rotation axis. Increasing values of V produce helical perturbations of the vortex lines around their low-V configuration. The situation has been compared by Donnelly[2,10] to magnetic systems, where the external field H contributes to the orientation of magnetic dipoles, while the temperature T has a disordering effect.

This interplay between orientation and disorder is expressed, in the simplest model of magnetism of 1/2 spin systems, by

$$M=N\mu\tanh\left[\frac{\mu H}{k_BT}\right], \tag{6.2}$$

μ being the magnetic moment of one particle, N the number of particles, k_B the Boltzmann constant, and M the total magnetization of the sample. This representation of the competition between order and disorder we have ascribed by the factor

$$\tanh\left[\frac{\sqrt{k\Omega}}{V}-C\right]. \tag{6.3}$$

in the proposal (6.1) for m, because Ω contributes to order and V to disorder.

In this model, the critical value V_{c1} of the velocity is given by

$$V_{c1}=\frac{1}{C}\sqrt{\kappa\Omega}, \tag{6.4}$$

which gives the physical way to measure the coefficient C. Using the experimental values of V_{c1} ($V_{c1}=0.053\sqrt{\Omega}$ cm sec$^{-1/2}$), it is seen that

$$C=0.596. \tag{6.5}$$

Of course, instead of tanh one could consider the Langevin function in classical paramagnetism, or other functions arising in paramagnetism of particles with other values of the spin. The essential fact, common to all of them, is that they go from -1 for high negative values of H to $+1$ for high positive values of H, in a relatively narrow range of temperature.

The coefficients A and B can be determined from the following considerations: for a given value of Ω, for small values of V, the tangle will be completely oriented along the rotation axis, and $m=A-B=1$. On the other side, when $V \gg V_{c1}$ (i.e. near V_{c2}) m assumes its higher value $m_0=1.009$ furnished by Eq. (5.6) or, in other terms, $A+B=m_0$. This indicates that

$$m=1+m_0\left\{1-\tanh\left[N\left(\frac{\sqrt{\kappa\Omega}}{V}-C\right)\right]\right\}. \tag{6.6}$$

Here, N is a phenomenological coefficient characterizing the rate of growth of L near V_{c1}. The experimental data do not allow us to determine it with a good approximation but they show simply that $N>20$.

In the microscopic model we have commented on, the second critical velocity V_{c2} is interpreted as the velocity where the helical vortex lines produced in V_{c1} have reached an amplitude of the order of the average vortex separation and have broken and reconnected, and form a disordered tangle.

We must observe that the data reported in Ref. 6 are obtained from experiments in which the second-sound wave is propagated orthogonal to the rotation axis, and the authors do not describe how they have taken into account the anisotropy of the tangle. This aspect is becoming increasingly studied in recent research.[1,7,12,14,15] In Ref. 7, the stationary value of another anisotropy coefficient $\langle \mathbf{s}'\cdot\hat{\mathbf{\Omega}}\rangle$ has been numerically determined, at the values $\Omega/2\pi=0.0079$ Hz and $V=0.08$ cm/s, which are relative to much smaller values of Ω and V than those considered in this work. Therefore, in Secs. V and VI, in the lack of availability of sufficient data on the dependence of the anisotropy coefficient from Ω and V, we have supposed that the values reported in Fig. 3 of Ref. 6 are the effective values of L. The results obtained will be close to the real situation as much as the data reported in (Ref. 6) correspond to the effective values of L. Further work on the microscopic bases should be carried out to understand the physical processes underlying the orientation of vortex lines in superfluid turbulence in the presence of rotation.

From this point of view, the recent proposal by Lipniacki,[12] where both the line length density L and the anisotropy vector $\mathbf{I}=\langle \mathbf{s}'\times\mathbf{s}''\rangle/\langle|\mathbf{s}''|\rangle$ are assumed as basic dynamical variables, instead of only L, seems very promising. Indeed, not only an evolution equation for $\mathbf{I}$ (related to the geometrical features of the vortices) is proposed, but also Vinen's equation (3.5) is modified, by taking into consideration the relative directions of the anisotropy vector $\mathbf{I}$ and the counterflow velocity $\mathbf{V}$. Lipniacki[12] shows that, in stationary counterflow situations, the vector $\mathbf{I}$ is parallel to the counterflow velocity $\mathbf{V}$ and obtains for L the following stationary value

$$L^{1/2}=\frac{c_1 I^{(H)}}{c_2^2\beta}, \tag{6.7}$$

where $I^{(H)}$ is the steady-state value of $I=|\mathbf{I}|$ in the presence of counterflow only, and $c_1=\langle|\mathbf{s}''|\rangle$, $c_2^2=\langle|\mathbf{s}''|^2\rangle$. Comparing with Eq. (1.2) we obtain

$$\gamma_H=\frac{c_1 I^{(H)}}{c_2^2\beta}. \tag{6.8}$$

Observe now that Eq. (4.7), which furnishes the stationary value of L for $V>V_{c2}$, can be written

$$L^{1/2}=\overline{\gamma}(V-V_{c2})+m\sqrt{\frac{2\Omega}{\kappa}} \tag{6.9}$$

and reduces to Eq. (6.7) in the absence of rotation, because when $\Omega=0$ also $V_{c2}=0$. Recalling that the coefficients α_i appearing in Eq. (3.9) depend on the anisotropy vector $\mathbf{I}$, we can say that $\overline{\gamma}$ is the value assumed by $\gamma(\mathbf{I})$ when Ω and V are simultaneously present:

$$\overline{\gamma}=\overline{\gamma}[\mathbf{I}(H,\Omega)]. \tag{6.10}$$

If we suppose that the coefficient $\gamma=\gamma(\mathbf{I})$ depend linearly on $\mathbf{I}$, we deduce that

$$\frac{I^{(H,\Omega)}}{I^{(H)}}=\frac{\overline{\gamma}}{\gamma_H} \tag{6.11}$$

and we can interpret $\overline{\gamma}/\gamma_H$ as an approximate value of the anisotropy of the disordered tangle induced by the rotation (for $V>V_{c2}$).

VII. CONCLUDING REMARKS

We have proposed a simple phenomenological model describing some of the most relevant observed effects in counterflow superfluid turbulence in the presence of rotation Ω. This model is based on a straightforward generalization [Eq. (3.10)] of Vinen's equation for the evolution of L. The generalized Vinen's equation is derived on dimensional grounds, but adding the effect of the rotation rate Ω; in absence of rotation it reduces to Vinen's equation. This generalized equation describes in a straightforward way some of the characteristic features which the presence of rotation imposes on the counterflow experiments.

It turns out that the combined effects of rotation and counterflow are rather subtle: on the one side, they are not merely additive; on the other side, for small V and Ω the combined effect is an extra production of vortices, whereas, for high values of V and Ω it inhibits the formation of vortices.

Such a model describes the critical velocity V_{c2} from a horizontal to a tilted straight line in L as a function of V^2. To

include the critical velocity V_{c1}, where L exhibits a small step, we suggest to complement this model with a mathematical hypothesis for one of the coefficients, inspired by an analogy between magnetic moments and vortex lines under rotation proposed by Donnelly:[4,11] in vortex lines, the rotation provides orientation and the velocity (heat flux) provides randomization; in magnetic moments, the magnetic field provides orientation and temperature provides randomization. A quantitative detailed description would require a deeper knowledge of the physical processes underlying the orientation of vortex lines, in combined counterflow and rotation, for which very recent numerical simulations[7] could provide a basis.

The meaning of both critical velocities V_{c1} and V_{c2} deserves some discussions. For $V<V_{c1}$, L is almost independent of V, showing only a small step change near V_{c1}. At $V>V_{c2}$, L becomes an affine function of V^2. The transition at V_{c2} has been studied in Secs. IV and V. For $V>V_{c2}$, the turbulence is characterized by a tangle of interconnected vortices, whereas for $V<V_{c2}$ the vortices form a somewhat ordered array of straight vortex lines ($V<V_{c1}$) or of helical lines with increasing amplitude ($V_{c1}<V<V_{c2}$). In all three regions may be said that the superfluid is turbulent, because vortices are present in all of them. However, from the point of view of the topology of the vortex lines, there is a sudden increase of complexity at $V=V_{c2}$, in comparison with the relatively ordered framework of lines for $V<V_{c2}$. The numerical simulation of Ref. 7 (see especially Fig. 2) are very illuminating in this respect, in the description of the evolution of a set of parallel vortex lines ($V<V_{c1}$), to parallel helices ($V_{c1}<V<V_{c2}$), to a reconnected tangle ($V>V_{c2}$). The topological difference in the transitions at V_{c1} and V_{c2} is reflected in the present phenomenological work on the different kind of analysis for both transitions in Secs. VI and IV, respectively.

ACKNOWLEDGMENTS

This work was supported by MIUR under grant ''Nonlinear mathematical problems of wave propagation and stability in models of continuous media'' and by founds 60%. D.J. was supported by the Spanish Ministry of Science and Technology under Grant No. BFM 2000-0351-003-0, and the Direcció General de Recerca of the Generalitat of Catalonia under Grant No. 2001 SGR 000186. He also acknowledges the support of G.N.F.M. of C.N.R. of Italy during his stay in Palermo University.

[1] A. P. Finne *et al.*, Nature (London) **424**, 1022 (2003).
[2] W. F. Vinen and J. J. Niemela, J. Low Temp. Phys. **128**, 167 (2002).
[3] R. J. Donnelly, *Quantized Vortices in Helium II* (Cambridge University Press, Cambridge, 1991).
[4] R. J. Donnelly, J. Phys.: Condens. Matter **11**, 7783 (1999).
[5] *Quantized Vortex Dynamics and Superfluid Turbulence*, edited by C. F. Barenghi, R. J. Donnelly, and W. F. Vinen (Springer, Berlin, 2001).
[6] C. E. Swanson, C. F. Barenghi, and R. J. Donnelly, Phys. Rev. Lett. **50**, 190 (1983).
[7] M. Tsubota, T. Araki, and C. F. Barenghi, Phys. Rev. Lett. **90**, 205301 (2003).
[8] W. F. Vinen, Proc. R. Soc. London, Ser. A **240**, 493 (1957).
[9] D. Cheng, M. W. Cromar, and R. J. Donnelly, Phys. Rev. Lett. **31**, 433 (1973).
[10] R. M. Ostermeir and W. I. Glaberson, J. Low Temp. Phys. **21**, 196 (1975).
[11] R. J. Donnelly, in *Quantized Vortex Dynamics and Superfluid Turbulence*, edited by C. F. Barenghi, R. J. Donnelly, and W. F. Vinen (Springer, Berlin, 2001), p. 31.
[12] T. Lipniacki, Phys. Rev. B **64**, 214516 (2001).
[13] S. K. Nemirovskii and W. Fiszdon, Rev. Mod. Phys. **67**, 37 (1995).
[14] C. F. Barenghi, S. Hulton, and D. C. Samuels, Phys. Rev. Lett. **89**, 275301 (2002).
[15] T. Araki, M. Tsubota, and C. F. Barenghi, Physica B **329-333**, 226 (2003).